

- friction measurements on reflective surfaces using nematic liquid crystal. *Exp. Fluids* **28**: 64–73.
- CARLING, P. A. 1992. The nature of the fluid boundary layer and the selection of parameters for benthic ecology. *Freshw. Biol.* **28**: 273–284.
- CHOW, V. T. 1959. *Open-channel hydraulics*. McGraw-Hill.
- DADE, W. B., A. J. HOGG, AND B. P. BOUDREAU. 2001. Physics of flow above the sediment-water interface, p. 4–43. *In* B. P. Boudreau and B. B. Jørgensen [eds.], *The benthic boundary layer*. Oxford Univ. Press.
- DAVIS, J. A. 1986. Boundary layers, flow microenvironments and stream benthos, p. 293–312. *In* P. De Deckker and W. D. Williams [eds.], *Limnology in Australia*. Junk.
- DITTRICH, A., AND U. SCHMEDTJE. 1995. Indicating shear stress with FST-hemispheres—effects of stream-bottom topography and water depth. *Freshw. Biol.* **34**: 107–121.
- FERNHOLZ, H. H., G. JANKE, M. SCHÖBER, P. M. WAGNER, AND D. WARNACK. 1996. New developments and applications of skin-friction measuring techniques. *Meas. Sci. Technol.* **7**: 1396–1409.
- FINELLI, C. M., D. D. HART, AND D. M. FONSECA. 1999. Evaluating the performance of an acoustic Doppler velocimeter in near-bed flows. *Limnol. Oceanogr.* **44**: 1793–1801.
- FRUTIGER, A., AND J. L. SCHIB. 1993. Limitations of FST hemispheres in lotic benthos research. *Freshw. Biol.* **30**: 463–474.
- GUST, G. 1988. Skin friction probes for field applications. *J. Geophys. Res.* **93C**: 14121–14132.
- HANRATTY, T. J. 1991. Use of the polarographic method to measure wall shear stress. *J. Appl. Electrochem.* **21**: 1038–1046.
- , AND J. A. CAMPBELL. 1983. Measurement of wall shear stress, p. 559–615. *In* R. J. Goldstein [ed.], *Fluid mechanics measurements*. Hemisphere.
- HARITONIDIS, J. H. 1989. The measurement of wall shear stress, p. 229–261. *In* M. Gad-el-Hak [ed.], *Advances in fluid mechanics measurements*. Springer.
- HART, D. D., B. D. CLARK, AND A. JASENTULYANA. 1996. Fine-scale field measurements of benthic flow environments inhabited by stream invertebrates. *Limnol. Oceanogr.* **41**: 297–308.
- MANGA, M., AND J. W. KIRCHNER. 2000. Stress partitioning in streams by large woody debris. *Water Resour. Res.* **36**: 2373–2379.
- NECE, R. E., AND J. D. SMITH. 1970. Boundary layer stress in rivers and estuaries. *J. Waterw. Harb. Res.* **96**: 335–358.
- NOWELL, A. R. M., AND P. A. JUMARS. 1984. Flow environments of aquatic benthos. *Annu. Rev. Ecol. Syst.* **15**: 303–328.
- PORTER, E. T., L. P. SANFORD, AND S. E. SUTTLES. 2000. Gypsum dissolution is not a universal integrator of ‘water motion’. *Limnol. Oceanogr.* **45**: 145–158.
- PRESTON, J. H. 1954. The determination of turbulent skin friction by means of Pitot tubes. *J. R. Aeronaut. Soc.* **58**: 109–121.
- ROBERTSON, A. L., J. LANCASTER, L. R. BELYEA, AND A. G. HILDREW. 1997. Hydraulic habitat and the assemblage structure of stream benthic microcrustacea. *J. N. Am. Benthol. Soc.* **16**: 562–575.
- STATZNER, B., AND R. MULLER. 1989. Standard hemispheres as indicators of flow characteristics in lotic benthos research. *Freshw. Biol.* **21**: 445–459.
- TAHERI, M., AND G. M. BRAGG. 1992. A study of particle resuspension in a turbulent flow using a Preston tube. *Aerosol Sci. Tech.* **16**: 15–20.
- TOMINAGA, A., AND I. NEZU. 1992. Velocity profiles in steep open-channel flows. *J. Hydraul. Eng.* **118**: 73–90.
- WHITE, F. M. 1999. *Fluid Mechanics*. 4th ed. McGraw Hill.
- WILCOCK, P. R. 1996. Estimating local bed shear stress from velocity observations. *Water Resour. Res.* **32**: 3361–3366.
- WINTER, K. G. 1977. An outline of the techniques available for the measurement of skin friction in turbulent boundary layers. *Prog. Aerospace Sci.* **18**: 1–57.

Received: 23 October 2000
Amended: 24 August 2001
Accepted: 28 August 2001

The optics of chromophoric dissolved organic matter (CDOM) in the Greenland Sea: An algorithm for differentiation between marine and terrestrially derived organic matter

Abstract—The optics of chromophoric dissolved organic matter (CDOM) in the Greenland Sea were investigated and compared to results from earlier studies in the Southeastern North Sea. Absorption at 375 nm (a_{375}) in the Greenland Sea varied from 0.77 m^{-1} to the detection limit of our instrument (0.05 m^{-1}), with the highest values found during summer. The spectral slope coefficient (S) ranged from 8.2 to 26.4 μm^{-1} with the highest values occurring during winter. Seasonal variations in the in situ production and degradation of CDOM were shown to be responsible for the trends seen. A negative correlation between S and a_{375} was evident in the Greenland Sea and differed noticeably from that found in coastal waters. The differing S - a_{375} behavior of CDOM known to be of terrestrial origin allowed the development of an algorithm for the differentiation between marine and terrestrial organic matter. The behavior of marine CDOM was modeled by $S = 7.4 + 1.1/a_{375}$.

Chromophoric dissolved organic matter (CDOM) exists in all natural waters. Its source is the degradation of plant ma-

terial of both terrestrial and aquatic origin (Kirk 1994). In coastal waters it is present in large quantities due to runoff from rivers and it is responsible for a major part of the attenuation of photosynthetically available radiation (PAR). Although it exists at substantially lower concentrations in oceanic environments, it still plays a significant role for the attenuation of light in the water column. The absorption of light by CDOM is strongest in the UV region and approaches zero with increasing wavelength. The behavior can be modeled using this exponential equation,

$$a_{\lambda} = a_{\lambda_0} e^{S(\lambda_0 - \lambda)} \quad (1)$$

where a_{λ} and a_{λ_0} are the absorption coefficients at a certain wavelength and a reference wavelength, respectively, and S is the spectral slope coefficient that determines the shape of the absorption curve (Jerlov 1968; Lundgren 1976; Bricaud et al. 1981).

CDOM's light absorption properties can result in both a positive and a negative feedback on aquatic organisms. In

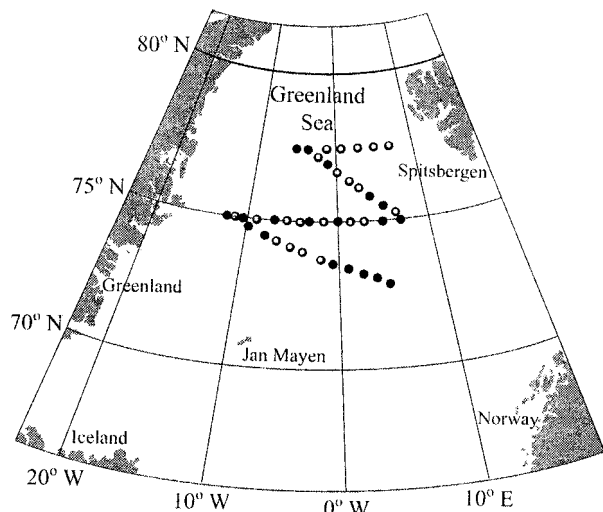


Fig. 1. A map of the study area and sampling stations for the Global Change program. The stations where CDOM samples were taken are shown with a filled circle.

surface layers harmful UV light is attenuated, while deeper in the water column light is limited (Arrigo and Brown 1996). The presence of CDOM also has to be taken into account before the water color signal can be used in remote sensing applications (Tassan 1988; Carder et al. 1989). The composition of CDOM is modified as it ages due to removal and modification of different fractions via adsorption on to particles, precipitation, bacterial degradation, and photo-oxidation (Brown 1977). These processes have in turn been shown to alter the optical properties of CDOM (Morris and Hargreaves 1997; Gao and Zepp 1998).

The Greenland Sea is a region of particular interest in oceanography because it is the site of North Atlantic Bottom Water (NABW) formation. The seasonal cooling initiates convective sinking of surface waters to the ocean depth. This is one of the driving forces in the global thermohaline circulation, which has considerable control over Earth's climate (Broecker 1997) and the global carbon cycle. There is an ongoing debate about how much of the DOM pool has its origin from land and how much is produced autochthonously in the marine environment both in coastal areas and in the open oceans, like the Greenland Sea (Wheeler et al. 1997; Opsahl et al. 1999). The differentiation has previously been quantified by in-depth chemical analyses (e.g., Opsahl et al. 1999). The objective of the present study was to characterize the optical properties of CDOM in the Greenland Sea and to develop an algorithm that can distinguish between CDOM of marine and terrestrial origin, respectively. The algorithm is based on the relationship between absorption and the slope parameter, S . Definition of the relationship for different regions will also aid in the development of regional algorithms for remote sensing applications. The CDOM data presented here are part of the Danish Global Change project, which is focused on studying carbon cycling in the North Atlantic Ocean.

Methods—Three cruises were undertaken in the same region of the Greenland Sea during November 1998, June 1999, and August 1999 (Fig. 1). A total of 195 samples were taken from

a range of depths from 5 to 3662 m. CDOM samples were filtered through a 0.2- μm Minisart syringe filter that had been prewashed with ultra pure Milli-Q water and 10 ml of sample before use and then stored refrigerated and in the dark in 100-ml amber glass bottles. The samples were analyzed in a spectrophotometer (Shimadzu UV-2401PC UV-Vis) after the cruises, approximately 1 month after sampling. Tests have shown that this method of storage has little or no effect on CDOM's absorption spectrum and is preferable to measurement onboard the ship, where the pitch, roll, and vibrations of the ship can considerably influence the quality of the spectra measured (unpubl. data). Reanalysis of 7-month-old samples showed no significant changes in absorption at 375 nm and a slight decrease in S by 1.61 μm^{-1} (~7% of mean S). Before the analysis, the samples were warmed to room temperature. CDOM's light absorption was measured in a 10-cm cuvette over the 300–800 nm range with 0.5 nm increments and referenced to ultra pure Milli-Q water. Effects on the spectra due to warming of the reference cuvette were eliminated by subtracting the spectra of Milli-Q blanks measured every tenth sample having the same temperature as the samples (i.e., room temperature).

The absorption coefficients were obtained by

$$A_{\lambda} = 2.303A_{\lambda}/L \quad (2)$$

where A_{λ} is the optical density at wavelength λ and L is the path length. CDOM's spectral properties were modeled from 300 to 650 nm using the equation

$$a_{\lambda} = a_{\lambda_0} e^{S(\lambda_0 - \lambda)} + K \quad (3)$$

where λ_0 was at 400 nm and K is a background constant that allows for any baseline shifts or attenuation not due to organic matter (Markager and Vincent 2000; Stedmon et al. 2000). The parameters a_{400} , S , and K were estimated simultaneously via a nonlinear regression of Eq. 3 using the secant (doesn't use derivatives) iterative method in SAS/STAT software package (SAS Institute Inc. 1994). This technique has been found to give a better fit of the model to the observed spectrum than the linear regression of log transformed data by preferentially weighting regions of higher CDOM absorption rather than the areas of low absorption (Stedmon et al. 2000). This method permits the use of a fixed wavelength range for estimating S and therefore simplifies the comparison of S values from CDOM in different environments. For example, S estimation is not influenced by the low signal found at wavelengths greater than 400 nm in oceanic waters. To demonstrate this, a dilution experiment was carried out to assess the impact of decreasing concentrations of CDOM on the regression estimation of the spectral slope coefficient (S). A 2-liter water sample was taken from the Sound between Sweden and Denmark, filtered, and then diluted. The salinity of the sample water was maintained constant during the dilutions by using a saline stock solution of Milli-Q water with the same salinity. A total of 25 dilutions were made, consisting of five different concentrations with five respective replicates.

Total organic carbon (TOC) was also measured during the Greenland Sea cruises. A total of 149 triplicate samples from a range of depths was analyzed. Samples were stored in 50-ml Nunclon® bottles (November and August cruises) or 10-ml Fritz sterile glass ampules (June cruise) in the cold and

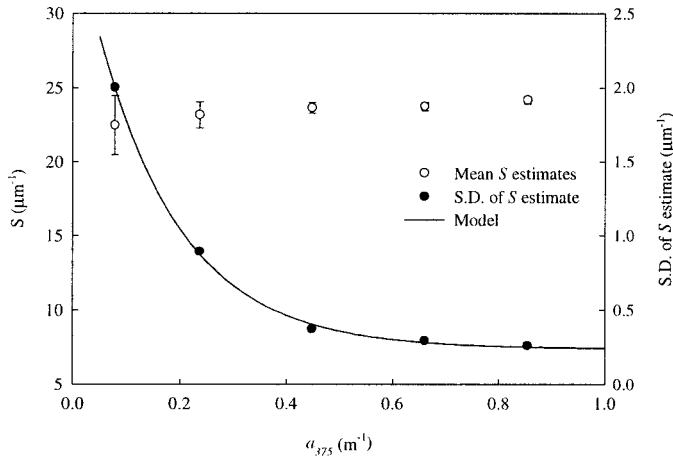


Fig. 2. The effects of the dilution of a CDOM sample with Milli-Q water (with the same salinity as the sample), on the estimation of S . The mean S estimates are shown, and the error bars show the standard deviation of the S at each concentration ($n = 5$). The second plot shows the increase in the standard deviations of S (filled squares) with decreasing a_{375} , which was subsequently modeled by $SD \text{ of } S = 0.24 + 2.9e^{-6.4a_{375}}$ ($r^2 = 0.998$).

dark, and preserved with 0.25 ml concentrated Suprapur® (Merck) HCl. The Nunclon® bottles were precleaned by soaking in 10% HCl overnight. The sample vessels were rinsed three times with sample water before filling. The samples were analyzed on a Shimadzu TOC5000 analyzer, which was calibrated before each batch was run with a four-point calibration curve using standard solutions of benzene-1,2-dicarboxylic acid ($r^2 = 1$ or 0.999). Blank values were subtracted from the measurements.

Results and discussion—The dilution experiment covered a range of CDOM concentrations with a_{375} ranging from 0.68 to 0.06 m^{-1} . The detection limit for the absorption measurements was found to be 0.05 m^{-1} . This was determined by doubling the standard deviation (2σ) of the spectra of five Milli-Q blanks. There were no noticeable changes in the standard deviations with wavelengths between 300–650 nm, and therefore the detection limit was calculated over and applies to the whole wavelength range. The mean S values for each dilution appeared to decrease slightly from 24.2 to 22.5 μm^{-1} with decreasing CDOM concentration (Fig. 2); however, an analysis of variance test showed the means did

not differ significantly from each other. There was an apparent decrease in the precision of the S estimates, as can be seen by looking at the standard deviations in Fig. 2. We found that this behavior could be closely modeled ($r^2 = 0.998$) by an exponential equation (Fig. 2). As the salinity of samples was maintained constant, and all samples were diluted and measured within the same day, we can attribute the behavior seen to limitations of the method of measurement rather than a salinity or bacterial degradation effect. In order to gain a better understanding of the effects of decreasing signal to noise ratio on the regression estimation of S , a Monte Carlo study was carried out. A series of absorption curves were calculated for a range of CDOM concentrations (a_{375} from 0.02 to 1.00 m^{-1}), according to Eq. 1, using an S coefficient of 24 μm^{-1} . A white noise signal was then generated using a random number procedure, adjusted to imitate the instrument noise (mean absorption of 0 m^{-1} and standard deviation of 0.025 m^{-1}), and added to the absorption curves. This resulted in a series of absorption curves with decreasing signal to noise ratios and a known original S value. These curves then underwent the nonlinear regression procedure for the estimation of S . As the concentration of CDOM decreased, the estimated S value tended to deviate more from its original value of 24 μm^{-1} . However, these deviations were relatively small, with the largest being 0.43 μm^{-1} at the lowest concentration. The overall mean estimate of S was 23.99 μm^{-1} (SD = 0.12 μm^{-1} , $n = 55$). It is evident that low absorption values themselves do not have a significant effect on the accuracy of S estimation but do, however, effect the precision of the S estimate. The uncertainty introduced by low absorption values was larger in the dilution experiment, most likely due to experimental errors. The model of the decline in precision from the dilution experiment (Fig. 2) was used to predict the limitations of the methods used (e.g., instrument and regression technique), when studying the behavior of S in natural waters.

Table 1 presents the results from the three cruises in the Greenland Sea. The specific absorption coefficient (a_{375}^*) was calculated by normalizing a_{375} to the TOC concentration. According to the temperature–salinity definitions given in Swift and Aagaard (1981), the samples originated from seven different water masses in the region (Table 2). A maximum value for a_{375} of 0.77 m^{-1} was found during the June 1999 cruise, and the range of values measured during this cruise was larger than for the other two cruises (Table 1). Mean

Table 1. Summary of CDOM data from the Greenland Sea cruises (this study) and the Skagerrak and North Sea (taken from Stedmon et al. 2000 and unpubl. data). S_{diff} is the mean difference between the measured and modeled S coefficient (Eq. 2). n/a = no data available.

Cruise	a_{375} (m^{-1})					S (μm^{-1})				a_{375}^* ($m^2 g^{-1} C$)					S_{diff}
	N	Mean	SD	Min	Max	Mean	SD	Min	Max	N	Mean	SD	Min	Max	(μm^{-1})
Global Change, Nov 98	20	0.07	0.01	0.05	0.11	20.16	2.52	17.20	26.41	18	0.12	0.02	0.08	0.16	−3.7
Global Change, Jun 99	107	0.16	0.12	0.05	0.77	16.51	3.52	8.22	24.08	80	0.23	0.18	0.07	1.27	−0.9
Global Change, Aug 99	67	0.16	0.07	0.06	0.37	16.22	2.97	9.75	23.23	51	0.19	0.09	0.08	0.56	0.3
Skagerrak, Feb 99	83	0.22	0.10	0.08	0.55	18.74	2.52	11.42	24.17	19	0.22	0.11	0.07	0.45	5.0
Skagerrak, Aug 99	20	0.47	0.26	0.24	1.29	20.03	3.05	11.31	22.79	n/a	n/a	n/a	n/a	n/a	9.2
SW North Sea, Feb 99	92	0.55	0.38	0.14	1.51	19.00	1.15	16.29	22.96	18	0.30	0.11	0.13	0.52	8.7
SW North Sea, Aug 99	68	0.51	0.23	0.13	1.02	19.62	1.61	16.45	27.97	n/a	n/a	n/a	n/a	n/a	9.7

Table 2. Water masses present according to definitions in Swift and Aagaard (1981). ASW = Arctic surface water, AW = Atlantic water, GSDW = Greenland Sea deep water, LAIM = lower Arctic intermediate water, NSDW = Norwegian Sea deep water, PW = Polar water, UAIM = upper Arctic intermediate water.

Cruise	Water masses sampled
Global Change, Nov 98	AW, GSDW, LAIM, NSDW, UAIM
Global Change, Jun 99	ASW, AW, GSDW, LAIM, NSDW, PW, UAIM
Global Change, Aug 99	ASW, AW, GSDW, LAIM, NSDW, PW, UAIM

a_{375} and S values for the June and August cruises were similar, and S agreed well with values reported from offshore saline waters by Green (1992). Analysis of variance (ANOVA) tests showed that the optical properties of CDOM (a_{375} , S , a_{375}^*) sampled during the two summer cruises were very similar to each other and both differed significantly ($P = 0.01$) from the winter data. In general the summer conditions were characterized by higher a_{375} and a_{375}^* values and lower S coefficients in comparison to winter conditions. The minimum values for S were very similar to those found by Mopper et al. (1996) in the central Pacific ocean (~600 m). In general a_{375}^* was lower than previously reported values (Stedmon et al. 2000, and references therein). The maximum values were found during the early summer cruise, and the mean for this period was analogous to that found in the Skagerrak (Stedmon et al. 2000). The lowest mean a_{375}^* was found during the winter cruise.

The mean a_{375} , S , and a_{375}^* values for the CDOM present in each water mass are shown in Table 3. A series of ANOVA tests was run to assess the variability of CDOM's optical properties with respect to water mass, season, and depth. Within the water masses present there were no significant differences in CDOM's optical properties between the two summer cruises. An exception was found in the Polar (PW) water mass where there was a significantly lower mean S in June than in August 1999 ($P = 0.05$). Comparison of CDOM samples originating from the Atlantic water mass (AW) and upper Arctic intermediate (UAIM) water mass during the three cruises showed that there were significant differences in the mean a_{375} , S , and a_{375}^* values between the summer and winter months (Table 3). This therefore suggests that the summer to winter variability reported earlier was not solely due to the presence of different water masses during the cruises. An ANOVA analysis was also carried out on the mean values within the photic zone, assumed to be from 0–50 m (0–3% surface light), and from the aphotic zone directly below (50–500 m) (Table 3). This shows that in general a_{375} and a_{375}^* in the surface waters were higher than in the deeper waters ($P = 0.05$). Further analysis of the individual cruise data showed that this was most significant during the June 1999 cruise (Table 3).

Figure 3 shows two representative examples of profiles taken in the Greenland Sea (refer to Fig. 1 for station positions). In the majority of circumstances a_{375} tended to decrease with depth and S showed a slight increase. From the examination of the profiles it was clear that S and a_{375} be-

Table 3. Mean values from each water mass and for the photic zone (0–50 m) and the aphotic zone (50–500 m). Refer to Table 2 for the full names of the water masses.

		a_{375} (m^{-1})			S (μm^{-1})		a_{375}^* ($m^2 g^{-1} C$)		
		<i>N</i>	Mean	SD	Mean	SD	<i>N</i>	Mean	SD
ASW	Total	9	0.19	0.07	15.9	3.0	7	0.19	0.06
	Jun 99	2	0.17	0.02	14.1	0.2	2	0.20	0.06
	Aug 99	7	0.20	0.08	16.4	3.3	5	0.19	0.07
AW	Total	18	0.14	0.07	18.3	4.3	13	0.17	0.05
	Nov 98	5	0.07	0.01	23.5	1.9	3	0.12	0.02
	Jun 99	8	0.15	0.05	16.9	3.3	7	0.18	0.04
	Aug 99	5	0.21	0.06	15.2	2.3	3	0.18	0.06
GSDW	Total	51	0.15	0.13	16.8	3.6	4	0.23	0.22
	Nov 98	5	0.07	0.01	19.1	1.9	5	0.12	0.03
	Jun 99	31	0.16	0.15	17.0	3.9	24	0.27	0.28
	Aug 99	15	0.15	0.08	15.6	3.0	15	0.20	0.13
LAIM	total	20	0.14	0.14	16.6	2.7	16	0.14	0.04
	Nov 98	1	0.08	n/a	17.8	n/a	1	0.13	n/a
	Jun 99	14	0.15	0.17	16.6	2.9	11	0.14	0.05
	Aug 99	5	0.14	0.05	16.3	2.6	4	0.13	0.04
NSDW	Total	42	0.13	0.07	17.0	3.3	31	0.22	0.12
	Nov 98	2	0.07	0.02	19.4	2.2	2	0.13	0.02
	Jun 99	29	0.13	0.08	16.9	3.5	20	0.25	0.14
	Aug 99	11	0.12	0.03	16.9	3.0	9	0.18	0.06
PW	Total	6	0.16	0.03	17.9	2.4	3	0.18	0.02
	Jun 99	4	0.17	0.02	16.5	0.7	2	0.19	0.02
	Aug 99	2	0.15	0.06	20.6	2.4	1	0.16	n/a
UAIM	Total	22	0.16	0.09	16.0	3.3	17	0.18	0.10
	Nov 98	4	0.07	0.01	19.5	1.6	4	0.11	0.02
	Jun 99	12	0.20	0.11	14.9	3.5	9	0.24	0.11
	Aug 99	6	0.15	0.04	15.8	2.3	4	0.12	0.03
Photic	Total	54	0.17	0.08	16.7	3.5	37	0.19	0.08
	Nov 98	5	0.08	0.02	21.6	3.3	4	0.13	0.03
	Jun 99	29	0.18	0.09	15.8	3.3	22	0.22	0.09
	Aug 99	20	0.19	0.06	16.9	2.9	11	0.17	0.06
Aphotic	Total	48	0.13	0.10	17.2	3.0	41	0.15	0.08
	Nov 98	8	0.07	0.01	20.4	2.4	7	0.11	0.02
	Jun 99	23	0.13	0.13	17.2	2.8	19	0.15	0.05
	Aug 99	17	0.15	0.06	15.7	2.4	15	0.17	0.12

haved inversely. Figure 4 shows the two parameters plotted against each other and the apparent inverse relationship. A similar relationship was also seen between a_{375}^* and S . Inverse relationships between a_{375} and S in marine waters have been reported before in the literature (Green 1992; Blough et al. 1993; Nelson and Guarda 1995; Vodacek et al. 1997; among others). However, care must be taken when studying the behavior of S in natural waters, as it is highly sensitive to the wavelength range over which it is estimated. It has been shown that S increases with decreasing wavelength (Kalle 1966; Carder et al. 1989; Coble and Brophy 1994; Markager and Vincent 2000). The use of variable wavelength ranges (e.g., 300 nm to the detection limit; Blough et al. 1993) results in a similar inverse relationship between a_{375} and S , as an artifact of the S estimation method.

Variability in S is associated with changes in the compo-

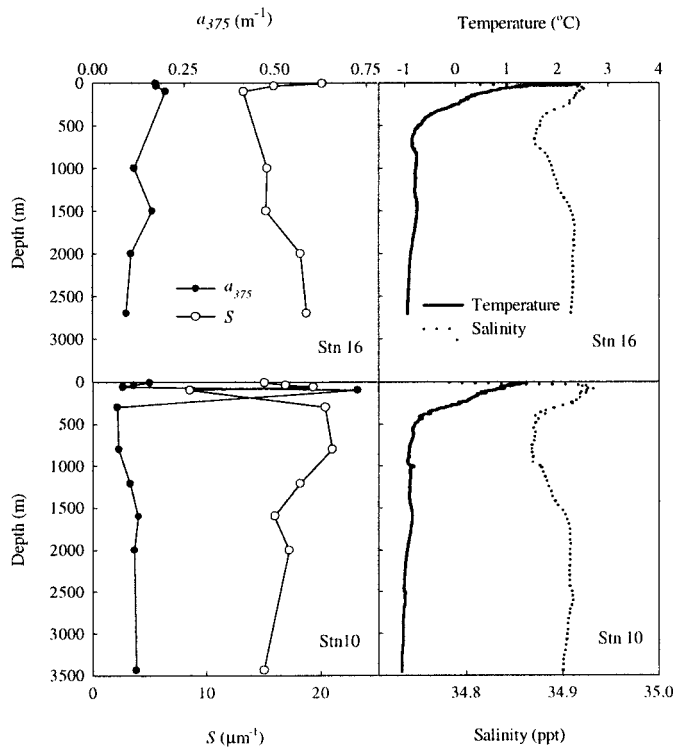


Fig. 3. Profiles of CDOM's optical properties (a_{375} , S), temperature, and salinity from Sta. 16, June 1999, and Sta. 10, August 1999. Refer to Fig. 1 for station positions.

sition of the CDOM pool (Carder et al. 1989). In the open ocean it is usually associated with degradation (solar and bacterial) and the mixing of different CDOM pools (Brown 1977; Gao and Zepp 1998). Work by Gao and Zepp (1998) and Morris and Hargreaves (1997) has shown that the photodegradation of terrestrially derived CDOM causes S to decrease. In contrast, results from a recent mesocosm study suggest that photoreactions of autochthonous CDOM cause S to increase as a_{CDOM} decreases (Whitehead et al. 2000).

A similar relationship between a_{CDOM} and S to that seen in the Greenland Sea data (Fig. 4) was reported by Del Castillo and Coble (2000) in samples from the Arabian Sea. The ranges in S seen in their study are alike to this study's, after differences in regression techniques used to calculate S are accounted for. The nonlinear technique used here is known to result in a 60% reduction in the variability of S estimates due to the increased precision of the estimate (Stedmon et al. 2000).

The variability of S in this study was reasonably large, which suggests a high degree of variability in the composition of CDOM in these waters. A similar variability of S at low CDOM concentrations off the Danish coast in the Skagerrak was reported by Stedmon et al. (2000). Figure 5 shows all the a_{375} and S data from the Greenland Sea plotted with the data from the Skagerrak and North Sea from the earlier studies (February 1999, Stedmon et al. 2000; and August 1999, unpubl. data). There is a clear overlap of some of the data from the Skagerrak deep waters with the Greenland Sea data, whereas data from the North Sea and the rest

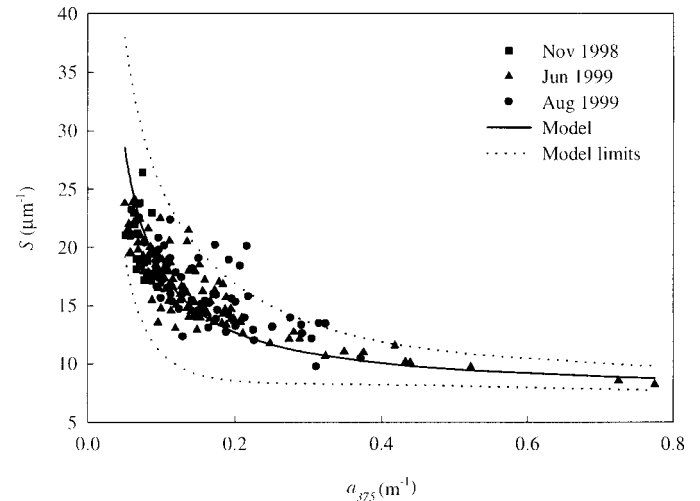


Fig. 4. CDOM data from the Greenland Sea during the November 1998, June 1999, and August 1999 cruises. Overlaid is the S - a_{375} model defined in the text with limits defined as ± 4 standard deviations of S from the model (precision of S estimate), calculated by using the equation in Fig. 2.

of the data from the Skagerrak do not exhibit the same behavior. Here, S stays relatively constant as a_{375} decreases. Using Fig. 5 one can clearly identify two different CDOM pools in these waters. There is the CDOM from coastal sources, with a comparatively invariant S value of approximately $18 \mu\text{m}^{-1}$, mixing with the North Sea waters. There is also an oceanic CDOM pool present in the Greenland Sea and Skagerrak deep waters, with intermediate a_{375} values and low S values that increase with falling concentrations. A fraction of the increased variability of S at low concentrations is due to the limitations of the method, evident from the results of the dilution experiment. However the lower

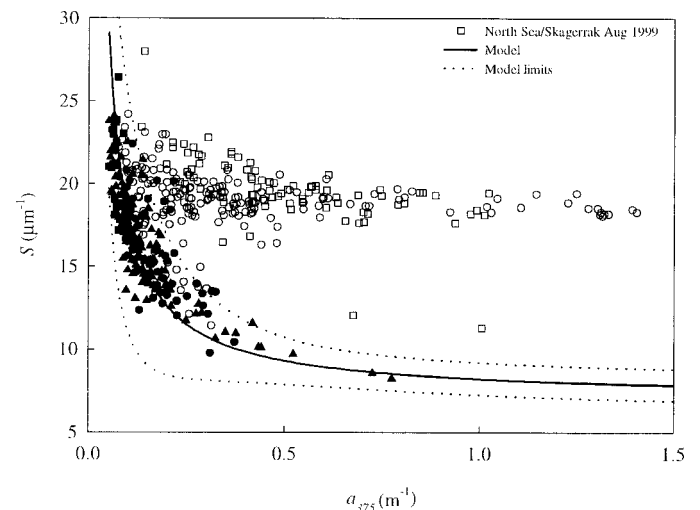


Fig. 5. CDOM data from the Greenland Sea (as in Fig. 4) plotted with data collected from the North Sea and Skagerrak in February 1999 (Stedmon et al. 2000) and August 1999 (unpubl. data). Data points that lie within the model limits are defined as autochthonous CDOM, while the rest is of terrestrial origin.

precision of the estimation of S at these concentrations cannot explain the general inverse relationship seen in the Greenland Sea data (Fig. 2). One would expect a bidirectional variability in S if this were the case.

It seems likely that in the Greenland Sea a variable low intensity oceanic source is present over a background pool of refractory CDOM. The results from the ANOVA tests show that there are seasonal fluctuations in CDOM abundance with the lowest values found in winter. The fact that the mean a_{375} and a_{375}^* values are highest both in the surface (photic) waters and during summertime suggests that CDOM is closely linked to in situ productivity in these waters (Nelson et al. 1998). The higher a_{375}^* values indicate the presence of more recently produced CDOM with a relatively more intense color. The coupling to productivity is reasonable since there are considerable differences in the seasonal biomass concentrations and productivity of these waters, mainly as a result of seasonal changes in surface irradiance. The mean values for a_{375}^* in this study were lower than those found in coastal waters by Stedmon et al. (2000). This could be a result of a higher proportion of particulate organic carbon in coastal waters or could also suggest that terrestrially derived CDOM tends to be more colored than autochthonous CDOM. The reduction in a_{375} and increase in S during the winter months is most likely due to the lack of resupply and continual degradation of the CDOM pool. This is supported by the fact that there is a significant reduction in a_{375}^* from summer to winter, which suggests that the colored fraction of the organic carbon pool is bleached in this period.

As all the samples from the Greenland Sea lie on the same S/a_{375} line, it poses the theory that a single CDOM source is dominant in this area. The analogous S/a_{375} pattern and a_{375}^* values seen in the deep offshore waters of the Skagerrak by Stedmon et al. (2000) suggest that the dominant CDOM source there is similar to the source in the Greenland Sea and most likely organic material produced by marine plankton. Dissolved organic carbon studies in the Arctic Ocean and surrounding seas have concluded that despite the number of large rivers that supply the region, in situ production is the largest source of dissolved organic carbon (Wheeler et al. 1997). Lignin tracer studies in Arctic water masses have shown that the dissolved organic carbon in the Greenland Sea gyre contains a low amount of lignin oxidation products and was enriched in ^{13}C (Opsahl et al. 1999). From this it was deduced that terrestrial dissolved organic matter plays a relatively insignificant role in carbon cycling in the Greenland Sea.

These findings suggest that CDOM of marine origin has different optical properties to terrestrial CDOM and that absorption measurements can be used to distinguish between them, at least at a_{375} values above 0.2 m^{-1} (Fig. 5). Since there appeared to be source dependent relationships between S and a_{375} , we decided to model the inverse behavior of marine CDOM in order to (1) allow the distinction between marine and terrestrial organic matter based on optical observations, and (2) allow the prediction of S values of CDOM in the Greenland Sea from the measurement of the absorption at a single wavelength. Owing to the uneven spread of data points due to a larger proportion of the water samples originating from below the photic zone, special con-

sideration had to be taken during the regression. Use of a standard regression technique would not be suitable in this case as there would be too much weighting of the regression at the low concentrations where most of the data points lie. To counter this, we modeled the frequency distribution (f) of the data and weighted the regression to the inverse of f (SAS Institute Inc. 1994). The frequency distribution was modeled as

$$f = xe^{-ya_{375}} = 143e^{-8.90a_{375}} \quad (4)$$

and the nonlinear weighted regression of the a_{375} - S data gave

$$S = y_0 + b/a_{375} = 7.4 + 1.1/a_{375} \quad (5)$$

Combining this model with the one established earlier for the reduction in precision of S estimation at low a_{375} values, we were able to account for deviations from the model at low CDOM concentrations (Fig. 4). As a large majority of the data fell within 4 standard deviations (precision of S estimate) of the model (Fig. 5), this confidence bracket could then be applied to the whole data set in order to allow the identification of marine CDOM. In Fig. 5 one can see how the data is divided. The mean deviations in S from the model (S_{diff}) for each cruise are shown in Table 1. Six points from the Greenland Sea data were found to fall outside of the range defined by the model. Four of the points lay clearly outside the confidence limits of the model and were from Polar water (PW) and Arctic surface water (ASW) sampled during the August cruise. They can be best seen in Fig. 4a ($a_{375} \approx 0.2 \text{ m}^{-1}$, $S \approx 19 \mu\text{m}^{-1}$) where they deviate from the general pattern. If the model is assumed to describe the behavior of marine CDOM in the region, then these points indicate the presence of terrestrial CDOM. This corresponds well with the fact that any terrestrial CDOM in the region is most likely to be transported into the Greenland Sea from the Arctic Ocean, into which there is considerable seasonal river discharge. The remaining two points were only marginally outside the confidence limits. The majority of the points from the North Sea and Skagerrak had S values above $18 \mu\text{m}^{-1}$ and deviated noticeably from the model (Fig. 5). These most likely reflect samples heavily influenced by local terrestrial sources. A number of points can be seen to lie in between the marine and terrestrial patterns, and these probably represent samples containing a mixture of CDOM from both marine and terrestrial sources. At low concentrations and high S values it becomes difficult to distinguish between the different pools of CDOM due to the reduced precision of the S estimates.

It is also interesting to note the lower mean S_{diff} calculated for Skagerrak February 1999 data (Table 1). This is due to CDOM in the Skagerrak deep waters exhibiting a similar behavior to that in the Greenland Sea. The surface waters of the Skagerrak and North Sea are under the influence of local terrestrial input, whereas the deeper waters are more oceanic in character. The fact that there is not a noticeably lower mean S_{diff} in the August data set is due to the comparatively smaller number of deep-water samples taken. This idea is further supported by the calculated mean S_{diff} for the surface waters (<50 m) and deeper waters (>50 m) of the Skagerrak in February 1999, which are 7.2 and 2.1 respectively.

Overall it would appear that this relatively simple model

performs well, although more data from coastal and oceanic waters are needed to test and refine it. It must be noted, however, that the model performs best at values of $a_{375} > 0.1 \text{ m}^{-1}$. If the behavior observed in the Greenland Sea is found to be valid for marine derived CDOM in general, the model derived in this work will provide a useful algorithm for the first-order approximation of CDOM sources.

The results from previous studies combined with this study's results allow us to conclude that the major and variable fraction of the CDOM in the Greenland Sea is derived from autochthonous sources. The optical properties and abundance of CDOM in the Greenland Sea vary seasonally with respect to productivity in the water column and solar irradiance. As the autochthonous CDOM degrades, the spectral slope coefficient increases. These results and the data from the North Sea/Skagerrak show that it is possible to model and distinguish between terrestrial and marine CDOM in oceanic environments, using optical measurements only. This makes optical measurements a useful investigative tool in oceanic carbon cycling studies. The results also suggest that it is possible to estimate S in oceanic water from the knowledge of CDOM's absorption at a single wavelength, assuming no influence from terrestrial CDOM. This has important consequences for biooptical modeling of water color (e.g., remote sensing), where CDOM's color signal is an interference.

C. A. Stedmon¹ and S. Markager

National Environmental Research Institute
Department of Marine Ecology
P.O. Box 358
Frederiksborgvej 399, DK-4000 Roskilde, Denmark

References

- ARRIGO, K. R., AND C. W. BROWN. 1996. Impact of chromophoric dissolved organic matter on UV inhibition of primary productivity in the sea. *Mar. Ecol. Prog. Ser.* **140**: 207–216.
- BLOUGH, N. V., O. C. ZAFIRIOU, AND J. BONILLA. 1993. Optical absorption spectra of waters from the Orinoco River outflow: Terrestrial input of coloured organic matter to the Caribbean. *J. Geophys. Res.* **98**: 2271–2278.
- BRICAUD, A., A. MOREL, AND L. PRIEUR. 1981. Absorption by dissolved organic matter of the sea (yellow substance) in the UV and visible domains. *Limnol. Oceanogr.* **26**: 43–53.
- BROECKER, W. S. 1997. Thermohaline circulation, the Achilles heel of our climate system: Will man-made CO₂ upset the current balance? *Science* **278**: 1582–1588.
- BROWN, M. 1977. Transmission spectroscopy examinations of natural waters. C. Ultraviolet spectral characteristics of the transition from terrestrial humus to marine yellow substance. *Estuar. Coast. Mar. Sci.* **5**: 309–317.
- CARDER, K. L., R. G. STEWARD, G. R. HARVEY, AND P. B. ORTNER. 1989. Marine humic and fulvic acids: Their effects on remote sensing of ocean chlorophyll. *Limnol. Oceanogr.* **34**: 68–81.
- COBLE, P. G., AND M. M. BROPHY. 1994. Investigation of the geochemistry of dissolved organic matter in coastal waters using optical properties. *SPIE Ocean Optics XII* **2258**: 377–389.
- DEL CASTILLO, C. E., AND P. G. COBLE. 2000. Seasonal variability of the colored dissolved organic matter during the 1994–95 NE and SW monsoons in the Arabian Sea. *Deep-Sea Res.* **47**: 1563–1579.
- GAO, H. Z., AND R. G. ZEPP. 1998. Factors influencing photoreactions of dissolved organic matter in a coastal river of the southeastern United States. *Environ. Sci. Technol.* **32**: 2940–2946.
- GREEN, S. A. 1992. Applications of fluorescence spectroscopy to environmental chemistry. Ph.D. thesis, Woods Hole Oceanographic Institution/Massachusetts Institute of Technology.
- JERLOV, N. G. 1968. *Optical Oceanography*. Oceanography Series 5. Elsevier.
- KALLE, K. 1966. The problem of Gelbstoff in the sea. *Oceanogr. Mar. Biol. Annu. Rev.* **4**: 91–104.
- KIRK, J. T. O. 1994. *Light and photosynthesis in aquatic ecosystems*. 2nd ed. Cambridge Univ. Press.
- LUNDGREN, B. 1976. Spectral transmittance measurements in the Baltic, report 30. Institute of Physical Oceanography, Univ. Copenhagen.
- MARKAGER, S., AND W. VINCENT. 2000. Spectral light attenuation and the absorption of UV and blue light in natural waters. *Limnol. Oceanogr.* **45**: 642–650.
- MOPPER, K., Z. M. FENG, S. B. BENTJEN, AND R. F. CHEN. 1996. Effects of cross-flow filtration on the absorption and fluorescence properties of seawater. *Mar. Chem.* **55**: 53–74.
- MORRIS, D. P., AND B. R. HARGREAVES. 1997. The role of photochemical degradation of dissolved organic carbon in regulating the UV transparency of three lakes on the Pocono Plateau. *Limnol. Oceanogr.* **42**: 239–249.
- NELSON, J. R., AND S. GUARDA. 1995. Particulate and dissolved spectral absorption on the continental shelf of the south-eastern United States. *J. Geophys. Res.* **100**: 8715–8732.
- NELSON, N. B., D. A. SIEGEL, AND A. F. MICHAELS. 1998. Seasonal dynamics of colored dissolved material in the Sargasso Sea. *Deep-Sea Res.* **45**: 931–957.
- OPSAHL, S., R. BENNER, AND R. W. AMON. 1999. Major flux of terrigenous dissolved organic matter through the Arctic Ocean. *Limnol. Oceanogr.* **44**: 2017–2023.
- SAS INSTITUTE INC. 1994. *SAS/STAT User's Guide*, vol. 2, version 6, 4th ed. GLM-VARCOMP.
- STEDMON, C. A., S. MARKAGER, AND H. KAAS. 2000. Optical properties and signatures of chromophoric dissolved organic matter (CDOM) in Danish coastal waters. *Estuar. Coast. Shelf Sci.* **51**: 267–278.
- SWIFT, J. H., AND K. AAGAARD. 1981. Seasonal transitions and water mass formation in the Iceland and Greenland seas. *Deep-Sea Res.* **28A**: 1107–1129.
- TASSAN, S. 1988. The effect of dissolved yellow substance on the quantitative retrieval of chlorophyll and total suspended sediment concentration from remote measurements of water colour. *Int. J. Remote Sens.* **9**: 787–797.
- VODACEK, A., N. V. BLOUGH, M. D. DEGRANDPRE, E. T. PELTZER, AND R. K. NELSON. 1997. Seasonal variation of CDOM and DOC in the Middle Atlantic Bight: Terrestrial inputs and photooxidation. *Limnol. Oceanogr.* **42**: 674–686.
- WHEELER, P. A., J. M. WATKINS, AND P. L. HANSING. 1997. Nutrients, organic carbon and organic nitrogen in the upper water column of the Arctic Ocean: implications for the sources of dissolved organic carbon. *Deep-Sea Res.* **44**: 1571–1592.
- WHITEHEAD, R. F., S. DE MORA, S. DEMERS, M. GOSSELIN, P. MONFORT, AND B. MOSTAJIR. 2000. Interactions of ultraviolet-B radiation, mixing, and biological activity on photobleaching of natural chromophoric dissolved organic matter: A mesocosm study. *Limnol. Oceanogr.* **45**: 278–291.

¹ Corresponding author (cst@dmu.dk).

Acknowledgements

The authors would like to thank S. Hemmingsen, W. Martinsen, and L. Hemmingsen for their help in collecting and running the samples. We would also like to thank W. Vincent and two anonymous referees for their constructive comments on the manuscript. This work was funded by SNF Global Change Program 9700196 and the Danish Earth Observation Program, grant 9600667.

Received: 22 January 2001

Accepted: 13 July 2001

Amended: 27 August 2001